Available online at www.sciencedirect.com
ScienceDirect
Trans. Nonferrous Met. Soc. China 24(2014) 3645−3651
Transactions of Nonferrous Metals Society of China
www.tnmsc.cn

Molecular dynamics simulation of fracture behaviors of ⟨110⟩ tilt grain boundaries in γ-TiAl

Wen-juan ZHAO[1,2], Dong-sheng XU[3], Jing-wei ZHAO[4], Hao WANG[3]

1. Key Laboratory of Materials Design and Preparation Technology of Hunan Province, Xiangtan University, Xiangtan 411105, China;
2. School of Mechanical Engineering, Xiangtan University, Xiangtan 411105, China;
3. Institute of Metal Research, Chinese Academy of Sciences, Shenyang 110016, China;
4. School of Mechanical, Materials and Mechatronic Engineering, University of Wollongong, NSW 2522, Australia

Received 8 January 2014; accepted 10 April 2014

Abstract: Molecular dynamics (MD) simulations were carried out to study the fracture behaviors of several symmetric tilt grain boundaries in γ-TiAl bicrystals with ⟨110⟩ misorientation axes. Tensile deformation along direction perpendicular to grain boundary was simulated under various strain rates and temperatures. The results indicate that the relative orientation of the grains and the presence of certain atom units are two critical factors of the interface structure affecting the stress required for dislocation nucleation. Dislocations nucleate and extend at or near the symmetric tilt grain boundaries during the tensile deformation of Σ3 (111) 109.5°, Σ9 (221) 141.1° and Σ27 (552) 148.4° interfaces. For Σ27 (115) 31.6° and Σ11 (113) 50.5° interfaces, the interfaces fractured directly in a cleavage manner due to no dislocation emitted from the boundary. The tensile fracture mechanisms of the bicrystals are that micro-cracks nucleate at the grain boundary and propagate along the interface. The variance of crack propagation is whether there is accommodation of plastic region at the crack tips.

Key words: gamma TiAl alloy; tilt grain boundary; molecular dynamics; tensile deformation; fracture

1 Introduction

It is well known that the mechanical properties are largely controlled by the character and distribution of grain boundary (GB) in polycrystalline materials. For most of metallic materials, the intrinsic behaviors of the grain boundary during plastic deformation, such as atomic motion and interaction between interface and dislocations, can have important effect on interface mobility, ductility, crack nucleation and even corrosion [1−5]. Consequently, GB deformation mechanisms have attracted many researchers in recent years. However, GB deformation behavior is very hard to quantify experimentally since it is controlled by several factors that act simultaneously on very small length and time scales. At such time and length scales, atomic simulation serves as an effective tool to explore the relationships between GB structure change and interfacial failure mechanisms during deformation.

TiAl-based alloys have low densities and possess attractive mechanical properties at elevated temperatures. Therefore, they have become important materials for jet engine applications in recent years [6−8]. But the problem of their brittleness has not yet been solved at room temperature [9,10]. Lamellar structure composed of layered two phases is a typical microstructure in TiAl alloys, in which different GB and inter-phase interfaces with complex orientations exist [11,12]. γ-TiAl phase has the $L1_0$ structure, which is one of the main component phases for TiAl-based alloys. The co-existence of these complex interfaces has duplex effects on the mechanical properties in TiAl-based alloys. On one hand, the interface may induce the nucleation of dislocation emission during deformation and facilitate deformation; on the other hand, the blocking of mobile dislocations by the interface may reduce the deformability of the alloy.

In experimental investigation, the polysynthetically

Foundation item: Project (51201147) supported by the National Natural Science Foundation of China; Project (14JJ6016) supported by the Natural Science Foundation of Hunan Province, China; Project (INFO-115-B01) supported by the Informalization Construction Project of Chinese Academy of Sciences, China

Corresponding author: Wen-juan ZHAO; Tel: +86-13787031201; E-mail: wjzhao1024@xtu.edu.cn

DOI: 10.1016/S1003-6326(14)63510-X

twinned (PST) TiAl crystals were employed to study the effect of complex interfaces. A series of experimental work has been done to study the effect of γ/γ or γ/α_2 interfaces on mechanical properties [13−16]. For example, LU et al [15] studied the fracture behaviors of the PST crystals under tension perpendicular to the interface. They found that micro-cracks nucleated at the interfaces and extended quickly which caused fracture. Similar results were obtained in the experiments of two phase titanium aluminides by APPEL et al [16]. It was found that interfaces provided a high density of dislocation sources and nucleation centers for deformation twins. At the same time, dislocation motion was strongly impeded by the interfaces. However, it is difficult to fully understand the effect of interfaces just by experimental study of the PST TiAl crystals, because there are more complex orientations existing in the PST crystals than those of "true" monocrystalline TiAl crystals.

In this work, the influence of orientations and atomic structures of GBs on the deformation and fracture behaviors of γ-TiAl alloys was investigated using molecular dynamics and static relaxation. In order to reveal the deformation and fracture mechanisms on interface of various nature from atomic scales, the simulations were focused on tensile deformation of several symmetric tilt grain boundaries (STGB) in γ-TiAl bicrystals with the ⟨110⟩ misorientation axes.

2 Interface model and computational technique

The symmetric tilt boundaries in γ-TiAl bicrystals were generated from coincident site lattice (CSL) model, which was formed by rotations around ⟨110⟩ crystallographic axes. For boundaries with the $[1\bar{1}0]$ misorientation axis (z-direction), the misorientation angle was measured using the [001] direction as the reference (0°). The deformation of γ-TiAl bicrystals was modeled using the embedded-atom method (EAM) potential by FARKAS [17]. Periodic boundary conditions were employed in all directions. Thus a second interface was generated at the border of the simulation box in the tensile direction (y-direction). Both the interfaces had identical structures. The dimensions of the box in the x-directions (parallel to the GB) and z-directions were tested and considered adequately large to avoid interactions between the two parallel interfaces and other finite-size effects. In total, each bicrystal interface model contains 2×10^5–3×10^5 atoms.

Static calculations were used to determine the minimum energy interface configurations by a nonlinear conjugate gradient method. After this step, the interface model was equilibrated using MD in the NVT ensemble at the pressure of 0 Pa and temperatures in the range of 1−600 K. A Nosé−Hoover thermostat was applied for temperature control. Uniaxial tensile tests were then simulated at constant strain rates of 10^8 and 10^9 s^{-1}, which was applied in the y-direction (normal to the interface plane) with a time step of 10^{-15} s. The MD simulations were carried out by a code based on MD++, which was written by CAI [18].

3 Results and discussion

3.1 Behaviors of stress versus strain

It has been studied that GB energies of CSL boundaries can be considered a function of misorientation angle for the 0 K equilibrium structure of FCC GBs [19,20], and there are two deep cusps in the GB energy for high-angle boundaries with ⟨110⟩ crystallographic axes, namely, GBs of Σ11 (113) 50.5° and Σ3 (111) 109.5°. In this work, the above two GBs were investigated, and another three higher energy GBs of Σ27 (115) 31.6°, Σ9 (221) 141.1° and Σ27 (552) 148.4° were also simulated for comparison. Figure 1(a) shows the tensile stress−strain curves for the above five γ-TiAl bicrystal interfaces with ⟨110⟩ crystallographic misorientation axes during tensile deformation at 1 K and 10^9 s^{-1}. Due to the same variation tendency in the tensile curves of 10^8 s^{-1} in contrast to that of 10^9 s^{-1}, the stress−strain curves of 10^8 s^{-1} will not be present here for simplicity. As shown in Fig. 1(a), first, the tensile peak stress of Σ11 (113) 50.5° GB is the highest one among the five interfaces, and the tensile peak stress of Σ27 (552) 148.4° GB is the lowest one. Moreover, the peak stress of Σ3 (111) 109.5° GB is much higher among the three interfaces of which misorientation angles are larger than 90°. And the peak stress of Σ11 (113) 50.5° GB is much higher than that of Σ27 (115) 31.6° GB. Second, there are two types of variation tendency in tensile stress−strain curves of the five interfaces. For Σ3 (111) 109.5°, Σ9 (221) 141.1° and Σ27 (552) 148.4° GBs, the tensile stresses present a process of softening−hardening−fracture; while the tensile stresses of Σ27 (115) 31.6° and Σ11 (113) 50.5° GBs decrease quickly to fracture after the peak stress.

Therefore, the five interfaces can be divided into two classes based on the difference of their tensile stress−strain curves. One class is GBs of Σ3 (111) 109.5°, Σ9 (221) 141.1° and Σ27 (552) 148.4° as group I, of which misorientation angles are larger than 90°. And the other class is GBs of Σ27 (115) 31.6° and Σ11 (113) 50.5° as group II, of which misorientation angles are less than 90°. Obviously, the difference of tensile stress−strain curves of the two groups indicates that different deformation mechanism exists between the two groups.

The stress−strain curves of Σ9 (221) 141.1° GB at

different temperatures are shown in Fig. 1(b). It indicates that yield stress decreases with the increase of deformation temperature.

3.2 Microstructure evolution during tensile deformation

Figures 2−5 show the projected views of microstructure evolution of Σ3 (111) 109.5°, Σ9 (221) 141.1°, Σ27 (115) 31.6° and Σ11 (113) 50.5° GBs during tensile deformation. As shown in Figs. 2−5, atoms are colored according to their coordination numbers. The coordinate system is shown in Fig. 2(a), and all of the projected views is obtained along the $[1\bar{1}0]$ direction (z axis). The microstructure of Σ3 (111) 109.5° GB at

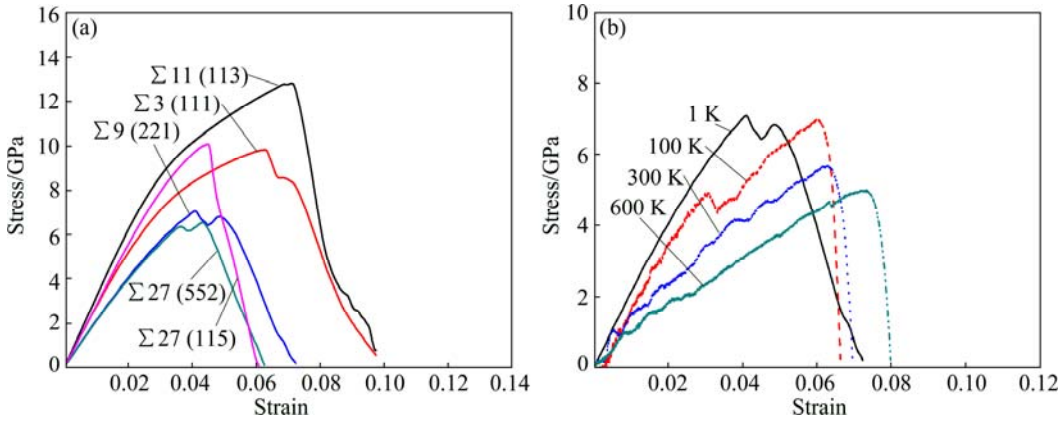

Fig. 1 Stress−strain curves of GB during tensile deformation: (a) Various GBs deformed at 1 K and 10^9 s^{-1}; (b) Σ9 (221) GB deformed at various temperatures

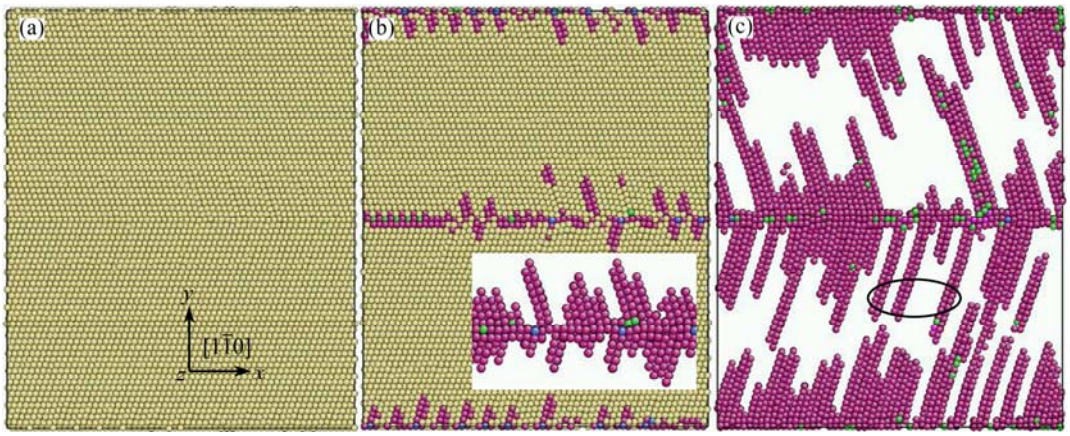

Fig. 2 Microstructural evolutions of Σ3 (111) 109.5° GB before and after stress peak when deformed at 1 K and 10^9 s^{-1}: (a) At stress peak; (b) Emission of dislocations from interface with inset showing local details; (c) Propagation of dislocations (Dislocations are marked by ellipse. Atoms are colored by coordination numbers in this and subsequent figures, and atoms with coordination number of 12 are made invisible in (b) and (c))

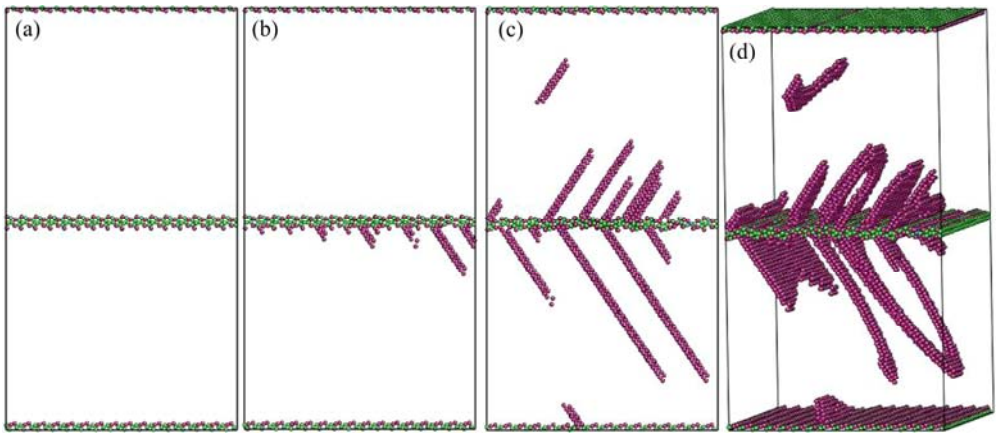

Fig. 3 Microstructural evolutions of Σ9 (221) 141.1° GB before and after stress peak when deformed at 1 K and 10^9 s^{-1}: (a) At stress peak; (b) Emission of dislocations from interface; (c) Propagation of dislocations; (d) 3D view of (c)

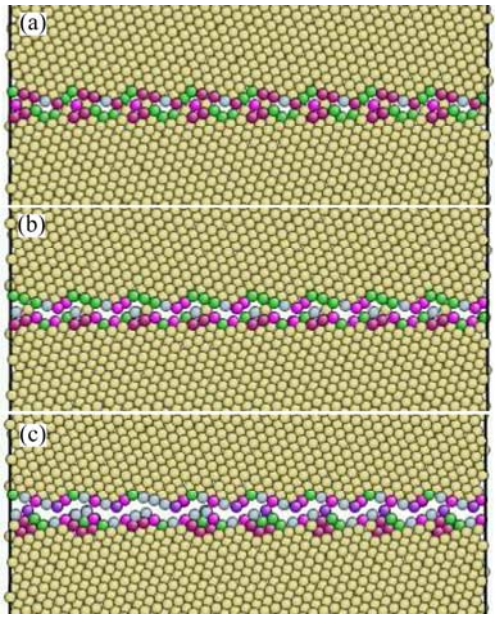

Fig. 4 Microstructural evolutions of Σ27 (115) 31.6° GB before and after stress peak deformed at 1 K and 10^9 s^{-1}: (a) At stress peak; (b) After stress peak; (c) Nucleation of micro-cracks

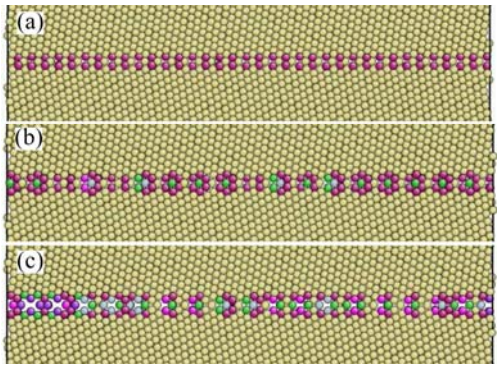

Fig. 5 Microstructural evolution of Σ11 (113) 50.5° GB before and after stress peak when deformed at 1 K and 10^9 s^{-1}: (a) At stress peak; (b) After stress peak; (c) Nucleation of micro-cracks

the interface holds equilibration state (Fig. 2(a)) before the stress reaches the peak value, and then partial dislocations nucleate from the interface (Fig. 2(b)). The dislocations are 1/6[112] $(11\bar{1})$ Shockley partial dislocations which slip on $(11\bar{1})$ plane. Subsequently, large quantity of dislocations emit and propagate from the interface (Fig. 2(c)), which leads to a rapid increase of the dislocation density. When dislocation slip is impeded by the second GB, the stress concentrates on the GB until the micro crack nucleates. The Σ9 (221) 141.1° and Σ27 (552) 148.4° GBs have the similar situations. The microstructure evolution of Σ9 (221) 141.1° GB is shown in Fig. 3.

Due to the emission of dislocations from the interface, stress relaxation occurs just after stress peaks for the three GBs (Group I). Thereafter, tensile stress has a narrow range of increase with increasing of the dislocation density. Finally, stress decreases quickly when micro cracks nucleate. The above phenomena agree well with the variation tendency of the stress−strain curves (Fig. 1(a)).

For Σ27 (115) 31.6° and Σ11 (113) 50.5° GBs (Group II), there is no dislocation nucleation during the whole tensile deformation process (Figs. 4−5), which has dramatic difference compared with the other three interfaces (Group I). Crack nucleation at the interface will be finally caused due to the stress concentration on the GB. Comparing tensile stress and microstructural evolution of the five GBs, it can be found that certain arrangement of atom units has important effect on them.

3.3 Crack nucleation and fracture mechanisms

Micro-cracks nucleate at the three GBs of Group I due to the stress concentration by accumulation of dislocations, as shown in Figs. 6(a)−(b). Plastic deformation zones are formed at or near the crack tips after the crack nucleates. As deformation proceeds, on one hand, new micro-cracks nucleate to release the stress accumulated along the grain boundary with the interaction of dislocations and GB; on the other hand, the cracks propagate perpendicular to the tensile direction under the applied stress. More and more cracks grow and link together, causing the final fracture of GB.

However, for Σ27 (115) 31.6° and Σ11 (113) 50.5° GBs (Group II), the bicrystals directly cleavage on the interface under the gradually increasing applied stress, as shown in Figs. 6(c)−(d). The flow stress increases and reaches a peak value and then decreases rapidly in a short time (Fig. 1(a)), which is a typical characteristic of brittle failure. The main reason is that there is no stress relieved by way of dislocation nucleation, and the stress concentration at grain boundary causes the delaminating of the interface.

3.4 Discussion

It shows that dramatic difference in superplastic deformation mechanisms and fracture behaviors of γ-TiAl bicrystal interfaces with various misorientation angles according to the above simulation results. Then, it was mainly discussed about the boundary structure, nucleation and propagation of micro-cracks and dislocations in the work.

First, it has been recognized that the particular atom arrangements of bicrystal interfaces play important role in the grain boundary energies of CSL symmetric tilt interfaces. Research on symmetric tilt interfaces of BCC and FCC metals [20−22] has shown that equilibrium grain boundary energy is a function of misorientation angle (arrangement of atom units) of the interface. The

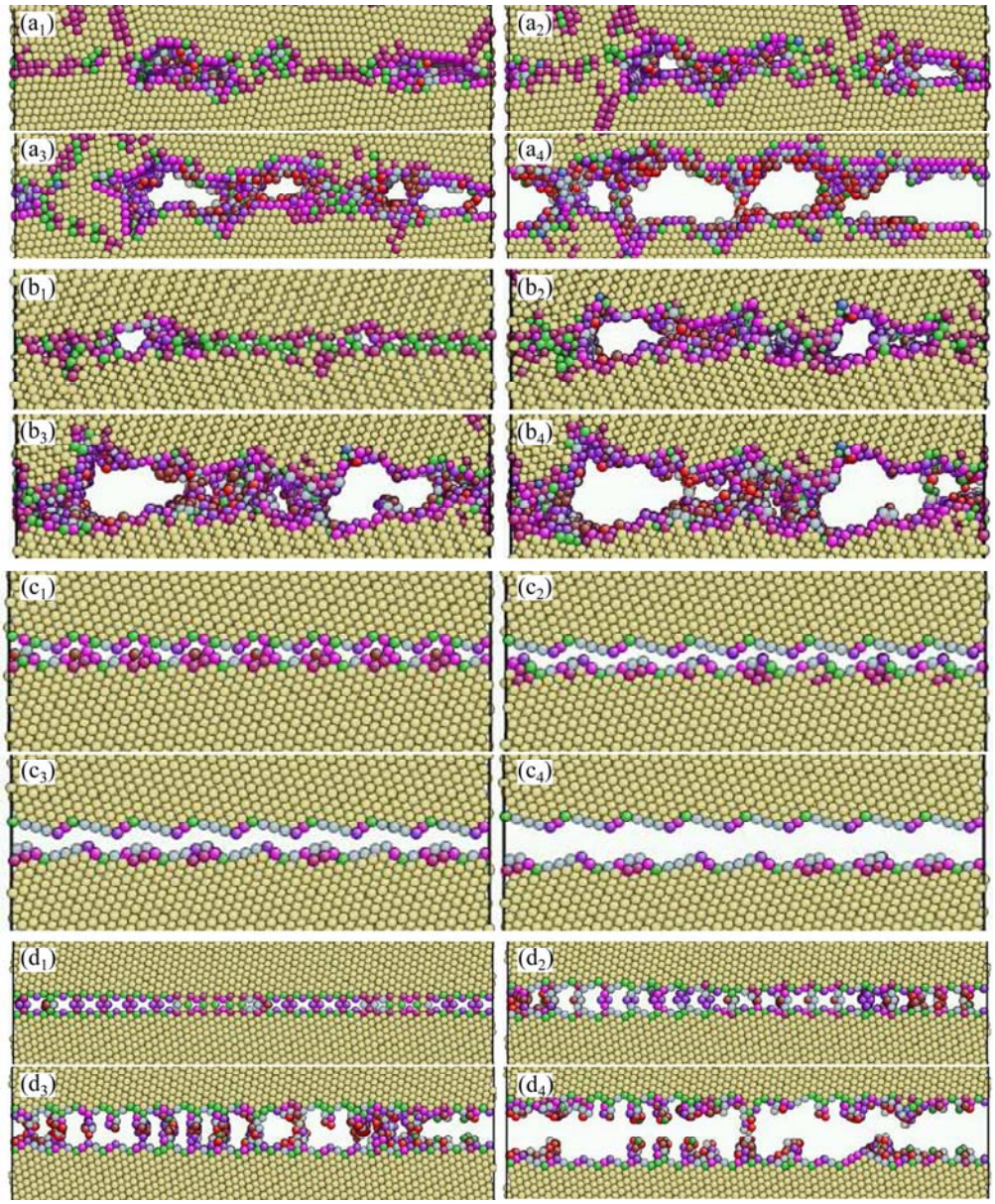

Fig. 6 Crack nucleation and propagation process of Σ3 (111) 109.5° GB (a_1−a_4), Σ9 (221) 141.1° GB (b_1−b_4), Σ27 (115) 31.6° GB (c_1−c_4) and (Σ11 (113) 50.5° GB (d_1−d_4) interfaces when deformed at 1 K and 10^9 s^{-1}

atomic structure of CSL symmetric tilt interface is composed of small units generally marked as alphabetical order (A, B, C, etc.). In this work, the atom units of Σ27 (115) 31.6°, Σ11 (113) 50.5 (Group II), Σ3 (111) 109.5°, Σ9 (221) 141.1° and Σ27 (552) 148.4° (Group I) GBs are ABC, CCC, DDD, EEE and EEA, respectively. Dramatic difference of grain boundary energy and mechanical properties was observed in above five interfaces just due to their particular arrangement of atom units, which was also found on Cu bicrystal interfaces by SPEAROT et al [23].

Furthermore, the effect of atomic structure on the mechanical properties was also observed on the microstructure evolution of the five interfaces during the tensile deformation. There is obvious dislocation nucleation and propagation observed during tensile deformation of the three interfaces of Group I (Figs. 2 and 3). It is essentially different from the interfaces of Group Ⅱ, because no dislocation nucleates during the whole tensile deformation (Figs. 4 and 5). It indicates that the particular arrangement of atom units at the grain boundary plays important role in the dislocation nucleation. That is, the stress required for dislocation emission is determined by the various arrangements of atom units at the grain boundary. As shown in Fig. 1(a) and Fig. 3, the peak tensile stress of Σ9 (221) 141.1° is lower than that of Σ27 (552) 148.4° GB, which is composed of E atom units. And partial dislocations obviously emit from the interface after they reach the peak tensile stress, demonstrating that the two interfaces

with E structural units could reduce the critical stress for dislocation nucleation. The similar appearance was observed in the calculation results of Al and Cu bicrystal interfaces by SANSOZ and MOLINARI [24] and ZHENG et al [25].

Therefore, the essential characteristic is whether dislocations emit during tensile deformation of the interfaces of Group I and II, which is the effect of various arrangements of atom units at the grain boundary. And the fracture behaviors have close relationship with stress concentration by way of dislocation accumulation and interaction of dislocations and grain boundary. For Σ27 (115) 31.6° and Σ11 (113) 50.5° GBs (Group II), there is no stress relieving by way of dislocation nucleation due to much higher critical stress for dislocation nucleation of the two interfaces. It leads that the bicrystal directly cleavages on the interface with rapid propagation of micro-cracks and no plastic zones formed at the crack tips.

4 Conclusions

1) The peak tensile stress of Σ11 (113) 50.5° GB is the highest one among the five interfaces, and that of Σ27 (552) 148.4° interface is the lowest one. For Σ3 (111) 109.5°, Σ9 (221) 141.1° and Σ27 (552) 148.4° GBs, the tensile stress presents a process of softening−hardening−fracture; while the tensile stresses of Σ27 (115) 31.6° and Σ11 (113) 50.5° GBs decrease quickly to fracture after the peak stress.

2) Dislocations nucleate at or near the symmetric tilt grain boundaries during the tensile deformation of Σ3 (111) 109.5°, Σ9 (221) 141.1° and Σ27 (552) 148.4°GBs. For Σ27 (115) 31.6° and Σ11 (113) 50.5° GBs, no dislocation emits from the boundary during the tensile deformation. The relative orientation of the grains and the presence of certain atom units are two critical factors of the interface structure affecting the stress required for dislocation nucleation.

3) Micro-cracks nucleate at the boundary due to the stress concentration by way of accumulation of dislocations for Σ3 (111) 109.5°, Σ9 (221) 141.1° and Σ27 (552) 148.4° GBs, and a large number of plastic deformations occur around the crack tips. By comparison, Σ27 (115) 31.6° and Σ11 (113) 50.5° GBs fracture directly in a cleavage manner. The variance of crack propagation depends on whether there is accommodation of plastic region at the crack tips.

References

[1] CHADWICK G A, SMITH D A. Grain boundary structure and properties [M]. London: Academic Press, 1976: 139−196.

[2] WOLF D. A model for ideal cleavage fracture of grain-boundaries in bcc metals [J]. Philosophical Magazine A, 1991, 63(6): 1117−1136.

[3] MISHIN Y, ASTA M, LI J. Atomistic modeling of interfaces and their impact on microstructure and properties [J]. Acta Materialia, 2010, 58: 1117−1151.

[4] ZHANG Y, ZHANG F C, QIAN L H, WANG T S. Atomic-scale simulation of α/γ-iron phase boundary affecting crack propagation using molecular dynamics method [J]. Computational Materials Science, 2011, 50: 1754−1762.

[5] LI X Y, WEI Y J, LU L, LU K, GAO H J. Dislocation nucleation governed softening and maximum strength in nano-twinned metals [J]. Nature, 2012, 464: 877−880.

[6] LU M. Investment casting of gamma titanium-aluminides for aircraft engine applications [J]. Structural Intermetallics, 2001, 2001: 225−232.

[7] DING H, ZHANG K F. Current status and developments in superplastic studies of materials [J]. The Chinese Journal of Nonferrous Metals, 2004, 14(7): 1059−1067. (in Chinese)

[8] ZHANG J, XIA K N. TiAl turbochargers for automobile application [J]. Light Metals Technology, 2009, 618−619: 559−562.

[9] GREENBERG B A, GORNOSTIREV Y N. Possible factors affecting the brittleness of the intermetallic compound TiAl. I. Transformations of dislocations to non-planar configurations [J]. Scripta Metallurgica, 1988, 22 (6): 853−857.

[10] KONG F T, LI B H, CHEN Y Y, HAN J C, ZHANG J W. Essence of room temperature brittleness of TiAl based alloys and improving approaches [J]. Journal of Advanced Materials, 2007, 39(1): 33−40.

[11] JIN Z, GRAY G T. Experimental determination of domain orientations and domain orientation relationships across lamellar interfaces in polysynthetically twinned TiAl crystals [J]. Materials Science and Engineering A, 1997, 231(1−2): 62−71.

[12] PEI Y L, SONG M, MA Y, GONG S K. Effects of heat shock at 800 °C on mechanical properties of gamma-TiAl alloys [J]. Intermetallics, 2011, 19(2): 202−205.

[13] KIM Y W, DIMIDUK D M. Progress in the understanding of gamma titanium aluminides [J]. JOM-Journal of the Minerals Metals & Materials Soceity, 1991, 43: 40−47.

[14] APPEL F, WAGNER R. Interface-related deformation phenomena in intermetallic gamma-titanium aluminides [J]. Physica Scripta, 1993, 49: 387−392.

[15] LU Y H, ZHANG Y G, QIAO L J,WANG Y B, CHEN C Q, CHU W Y. In-situ TEM study of fracture mechanisms of polysynthetically twinned (PST) crystals of TiAl alloys [J]. Materials Science and Engineering A, 2000, 289(1−2): 91−98.

[16] APPEL F, LORENZ U, SPARKA U, WAGNER R. The influence of lamellar interfaces on the mechanical properties of (alpha 2+gamma) titanium aluminides [J]. Strength of Materials, 1994, 973: 337−340.

[17] FARKAS D. Interatomic potentials for Ti−Al with and without angular forces [J]. Modelling and Simulation in Materials Science and Engineering, 1994, 2(5): 975−984.

[18] CAI W. Micro and Nano Mechanics: MD++[OL]. [2012−04−06]. http://web.stanford.edu/caiwei/Forum.

[19] RITTNER J D, SEIDMAN D N. ⟨110⟩ symmetric tilt grain-boundary structures in fcc metals with low stacking-fault energies [J]. Physical Review B, 1996, 54 (10): 6999−7015.

[20] CHANDRA N, DANG P. Atomistic simulation of grain boundary sliding and migration [J]. Journal of Materials Science, 1999, 34(4): 655−666.

[21] KRAKOW W. Real-time computer simulation of transmission electron-microscope images with tilted illumination-grain-boundary applications [J]. Journal of Electron Microscopy Technique, 1991, 19(3): 366−378.

[22] WOLF D, YAMAKOV V, PHILLPOT S R, MUKHERJEE A, GLEITER H. Deformation of nanocrystalline materials by molecular-dynamics simulation: Relationship to experiments [J]. Acta Materialia, 2005, 53: 1−40.

[23] SPEAROT D E, TSCHOPP M A, JACOB K I, MCDOWELL D L. Tensile strength of ⟨100⟩ and ⟨110⟩ tilt bicrystal copper interfaces [J]. Acta Materialia, 2007, 55: 705−714.

[24] SANSOZ F, MOLINARI J F. Mechanical behavior of Sigma tilt grain boundaries in nanoscale Cu and Al: A quasicontinuum study [J]. Acta Materialia, 2005, 53(7): 1931−1944.

[25] ZHENG Y G, ZHANG H W, CHEN Z, LU C, MAI Y W. Roles of grain boundary and dislocations at different deformation stages of nanocrystalline copper under tension [J]. Physics Letters A, 2009, 373(5): 570−574.

γ-TiAl 中⟨110⟩倾斜晶界断裂行为的分子动力学模拟

赵文娟[1,2]，徐东生[3]，赵敬伟[4]，王 皞[3]

1. 湘潭大学 材料设计及制备技术湖南省重点实验室，湘潭 411105；

2. 湘潭大学 机械工程学院，湘潭 411105；

3. 中国科学院 金属研究所，沈阳 110016；

4. School of Mechanical, Materials and Mechatronic Engineering, University of Wollongong, NSW 2522, Australia

摘 要：采用分子动力学(MD)方法研究 γ-TiAl 合金中⟨110⟩对称倾斜界面的断裂行为，模拟在不同温度与应变速率下垂直界面方向的拉伸变形。结果表明：晶粒的相对取向及晶界特定的原子结构是影响位错形核临界应力的两个主要因素。取向差角度大于 90°的 Σ3 (111) 109.5°、Σ9 (221) 141.1° 和 Σ27 (552) 148.4° 界面，位错在晶界处形核和扩展；取向差角度小于 90°的 Σ27 (115) 31.6° 和 Σ11 (113) 50.5°界面，无位错在晶界处形核，当应力达到峰值后界面直接断裂。γ-TiAl 双晶的断裂机制为微裂纹在界面处的形核及沿界面扩展；不同取向差界面的区别在于裂纹前端有无塑性区增韧。

关键词：γ-TiAl 合金；倾斜晶界；分子动力学；拉伸变形；断裂

(Edited by Chao WANG)